无 机 化 学 学 报

2021年　　第37卷　　第8期

目　次

综　述

论　文

勘　误

CHINESE JOURNAL OF INORGANIC CHEMISTRY

Vol.37 No.8 Aug. 2021

CONTENTS

Cover

Reviews

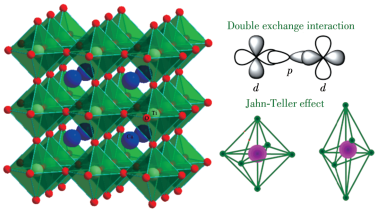

Based on the Jahn-Teller distortion effect and double exchange effect, the influence of doping on the microwave absorbing properties of perovskite was analyzed, and the existing perovskite microwave absorbing materials and their composites were summarized.

Articles

Synthesis, Crystal Structure and Properties of Mn(Ⅱ)/Co(Ⅱ) Coordination Polymers Based on 1,4-Bis(imidazol-1-yl)benzene (English)

YANG Xiao-Qing, HE Chun-Yu, ZHANG Yan-Hong, MU Xian-Gui, JIANG Shuang

DOI:10.11862/CJIC.2021.165
Chinese J. Inorg. Chem., **2021**,**37**(8):1364-1374

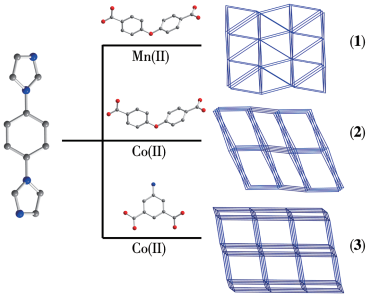

Three coordination polymers {[Mn_3(oba)$_3$(bib)(DMF)(H_2O)]·DMF}$_n$ (**1**), [Co(Hoba)$_2$(bib)]$_n$ (**2**), {[Co(aip)(bib)]·DMF}$_n$ (**3**) (bib=1,4-bis(imidazol-1-yl)benzene, H_2oba=4,4′-oxybisbenzoic acid, H_2aip=5-aminoisophthalic acid) have been synthesized. Compound **1** shows rapid and selective separation of Congo red from dye mixtures. Compounds **2** and **3** display weak antiferromagnetic interaction between the Co(Ⅱ) centers.

Reactivity of Half-Sandwich 16e Carborane Compound Cp*$CoS_2C_2B_{10}H_{10}$ with Phosphorous Compounds

YE Hong-De, ZHANG Xin-Yu, XIAO Xin, ZHU Qing-Rong, HE Lu-Ling, PENG Hua-Nan, LIU Zi-Wei

DOI:10.11862/CJIC.2021.109
Chinese J. Inorg. Chem., **2021**,**37**(8):1375-1380

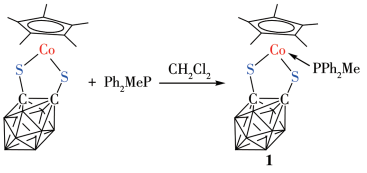

Half-sandwich 16e carborane complex Cp*$CoS_2C_2B_{10}H_{10}$ reacted with diphenylmethylphosphine to afford addition compound (Cp*$CoS_2C_2B_{10}H_{10}$)(PPh_2Me) (**1**). **1** has been characterized by IR, NMR, elemental analysis, mass spectrum and single-crystal X-ray diffraction analysis. The ultraviolet and fluorescent performances of **1** have also been determined.

Cu(Ⅱ)/ Zn(Ⅱ) Coordination Polymers Constructed by 3-(4′-Carboxy-phenoxy) benzoic Acid: Synthesis, Crystal Structure and as a Fluorescence Sensor to Acetone and Tb^{3+} Ion

LI Zhen-Hua, LUO LI-Lin, WAN Chong-Qing, HU Yue-Qi, ZHOU Ruo-Han, LI Xia

DOI:10.11862/CJIC.2021.177
Chinese J. Inorg. Chem., **2021**,**37**(8):1381-1389

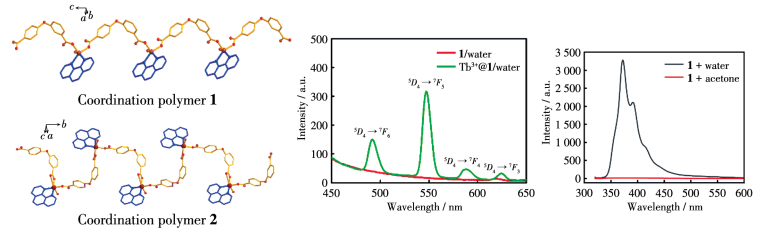

Two new coordination polymers, [Zn(3,4′-oba)(phen)(H_2O)]$_n$ (**1**) and [Cu(3,4′-oba)(phen)(H_2O)]$_n$ (**2**) (3,4′-H_2oba=3-(4′-carboxy-phenoxy)benzoic acid, phen=phenanthroline), were synthesized by hydrothermal method. Coordination polymer **1** can be used as a sensor for detecting acetone molecule and Tb^{3+} ion.

Effect of Component Control of Catalysts with Dual Ligand CuFe@MOFs as Precursor on Performance of CO_2 Hydrogenation to C_{2+} Alcohol

ZHANG Qian, WEN Yue-Li, WANG Bin, FAN He-Ming, YANG Chen, SONG Rong-Peng, ZHANG Wei-Zhong, HUANG Wei

DOI:10.11862/CJIC.2021.148
Chinese J. Inorg. Chem., **2021**,**37**(8):1390-1398

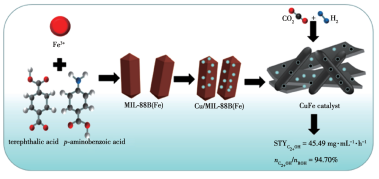

CuFe@MOFs derived catalyst $C_{5:2}$ (the molar ratio of terephthalic acid to *p*-aminobenzoic acid was 5∶2) with highest low-valence Fe species showed the best performance for CO_2 hydrogenation to C_{2+} alcohol (C_{2+}OH) that the space time yield (STY) of C_{2+}OH was 45.49 mg·mL^{-1}·h^{-1}.

Mn-Doped $LiFePO_4$ Cathode Material: Solvothermal Preparation and Electrochemical Performance

WU Xing-Yu, RUAN Ding-Shan, MAO Lin-Lin, FENG Mao-Hua, LI Bin

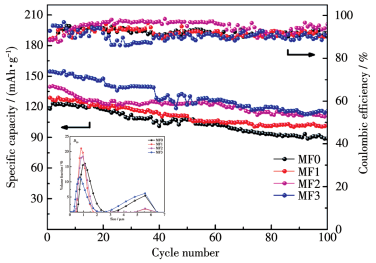

Mn-doped $LiFePO_4$ had smaller particle size and better electrochemical performance compared with pure phase $LiFePO_4$.

DOI:10.11862/CJIC.2021.144
Chinese J. Inorg. Chem., **2021**,**37**(8):1399-1406

Effect of Film Thickness of N-Doped Porous Carbon Loaded with Isolated Single Fe Atoms Counter Electrode on Dye-Sensitized Solar Cells Performance

ZHAO Kai-Feng, ZHANG Xiao-Yu, FU Yu-Hang, HAN Xiao, CAO Ying, LI Xiao-Ting, LI Ling

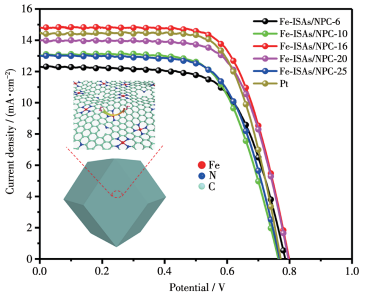

N-doped porous carbon (NPC) loaded with isolated single Fe atom (Fe-ISAs/NPC) was prepared through molecular cage-encapsulated-precursor pyrolysis. Meanwhile, film thickness of counter electrode effect on the performance of DSSCs was studied by electrochemical measurement.

DOI:10.11862/CJIC.2021.166
Chinese J. Inorg. Chem., **2021**,**37**(8):1407-1413

Secondary Crystallization and Passivation of Perovskite Film Induced by Dithizone Post-treatment

HOU Wen-Jing, MA Yu-Ting, HAN Gao-Yi

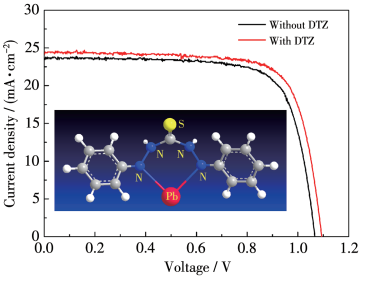

Dithizone (DTZ) post-treatment can improve the performances of organic-inorganic hybrid perovskite solar cells. DTZ can not only improve the morphology of the perovskite film by inducing its secondary crystallization, but also can passivate the Pb defects by forming the lewis acid-base adducts through covalent bond between nitrogen atoms and Pb^{2+}.

DOI:10.11862/CJIC.2021.182
Chinese J. Inorg. Chem., **2021**,**37**(8):1414-1420

Preparation of Nickel Foam Supported Fe_2O_3@Ni_3S_2 Nanowires Network Electrode and Electrocatalytic Oxygen Evolution Performance

QIAO Qing-Shan, ZHANG Sheng, ZHOU Xiao-Ya, HU Li-Bing, LU Hong-Bin, TANG Shao-Chun

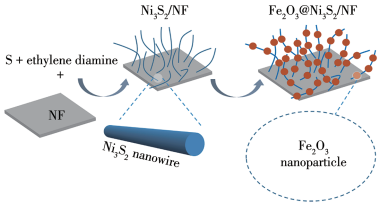

A Fe_2O_3@Ni_3S_2/NF (NF=nickel foam) nanocomposite structure was designed and prepared. The oxygen evolution reaction overpotential of the catalyst was only 223 mV at a high current density of 100 $mA\cdot cm^{-2}$.

DOI:10.11862/CJIC.2021.162
Chinese J. Inorg. Chem., **2021**,**37**(8):1421-1429

Two-Step Preparation of Quasi-Spherical α-Calcium Sulfate Hemihydrate from Flue Gas Desulphurization Gypsum (English)

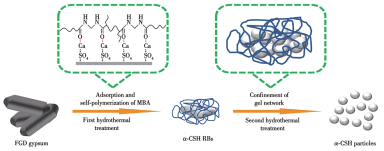

MA Wen-Jing, GAO Li-Li, LI Yun, CHEN Xue-Qing, GUO Hong-Fei, LI Zhi-Shui, CAO Ji-Lin

N,*N*′-methylenediacrylamide regulates the generation of small and quasi-spherical α-calcium sulfate from flue gas desulfurization (FGD) gypsum by preferential adsorption and self-polymerization to confine the growth of α-calcium sulfate.

DOI:10.11862/CJIC.2021.167
Chinese J. Inorg. Chem., **2021**,**37**(8):1430-1438

Preparation and Photocatalytic Activity of Holey Ultrathin g-C_3N_4 Nanosheets-Supported Pt Composite (English)

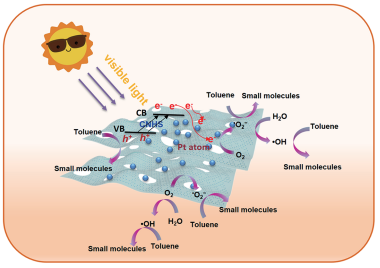

MA Shuai-Shuai, GU Jian-Dong, GAO Yuan, ZONG Yu-Qing, XUE Jin-Juan, YE Zhao-Lian

Pt-CNHS (CNHS=holey ultrathin g-C_3N_4 nanosheets) photocatalyst exhibited significantly enhanced photocatalytic activities toward gaseous toluene degradation and degradation rate was nearly 7.6 and 3.1 times higher than that of CNB (g-C_3N_4) and CNHS, respectively.

DOI:10.11862/CJIC.2021.164
Chinese J. Inorg. Chem., **2021**,**37**(8):1439-1448

Mn(Ⅱ)/Ni(Ⅱ) Complexes Based on 5-Methyl-1*H*-pyrazole-3-carboxylic Acid: Syntheses, Structures, Electrochemical and Luminescent Properties (English)

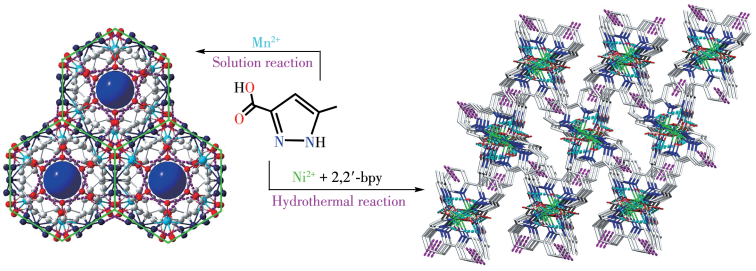

LIU Lu, CHENG Mei-Ling, TANG Li-Zhi-Peng, LIU Zheng, LIU Qi

Two new complexes, [Mn(HMPCA)$_2$(H_2O)$_2$] (**1**) and [Ni(HMPCA)$_2$(2,2′-bpy)]·2H_2O (**2**), with different 3D supramolecular structures, were obtained by assembling of Mn (Ⅱ)/Ni (Ⅱ) ions, 5-methyl-1*H*-pyrazole-3-carboxylic acid (H_2MPCA), in the absence/presence of 2,2′-bipyridine (2,2′-bpy). Electrochemical properties of **1** and **2** show that electron transfer of M(Ⅱ) between M(Ⅲ) (M=Mn and Ni) in electrolysis is quasi-reversible process. Two complexes displayed blue fluorescence in the solid state at room temperature.

DOI:10.11862/CJIC.2021.170
Chinese J. Inorg. Chem., **2021**,**37**(8):1449-1456

Synthesis of High-Performance and Low-Loading PtCo/C Proton Exchange Membrane Fuel Cell Catalysts (English)

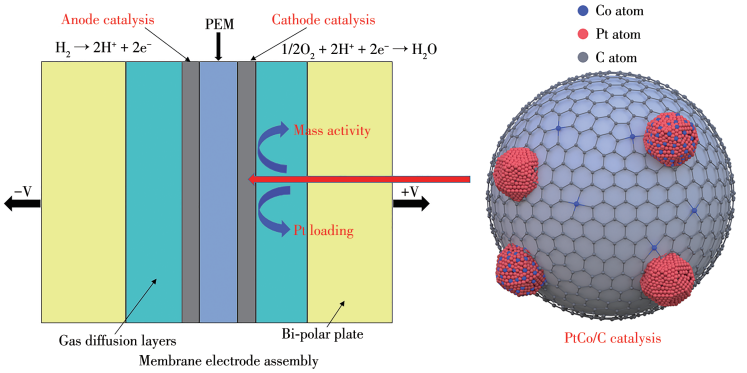

ZHAO Xu-Yan, WU Yu-En

DOI:10.11862/CJIC.2021.172
Chinese J. Inorg. Chem., **2021**,**37**(8):1457-1464

Effect of Ions on Photocatalytic Performance of UIO-66-2OH (English)

LI Shi-Xiong, HUANG Feng-Lan, BIN Yue-Jing, WEI Yu-Cai, TANG Xue-Li, LIAO Bei-Ling

DOI:10.11862/CJIC.2021.173
Chinese J. Inorg. Chem., **2021**,**37**(8):1465-1474

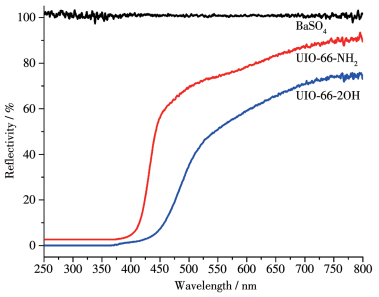

The UIO-66-2OH photocatalytic degradation rate of methylene blue at pH=3 was better than the reference catalyst UIO-66-NH_2. The ion coexistence experiments showed that the Fe^{3+}, HCO_3^-, and CO_3^{2-} can enhance the photocatalytic performance. But, Na^+, K^+, Ca^{2+}, Cu^{2+}, Cl^-, SO_4^{2-}, and PO_4^{3-} ions can inhibit the photocatalytic performance.

Controllable Synthesis of Metal-Organic Frameworks Mn-Fluorescein in One Pot for Magnetic Resonance/Optical Imaging (English)

GAO Xue-Chuan, ZHANG Man, SUN Xu-Jian, WANG Yue-Wu

DOI:10.11862/CJIC.2021.156
Chinese J. Inorg. Chem., **2021**,**37**(8):1475-1481

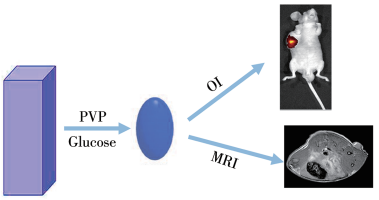

For the first time, magnetic resonance imaging (MRI) reagent and optical imaging (OI) reagent were focused on a simple MOFs via one-step method.

Synthesis of High-Flux Mordenite Membranes by Binary Cations System for Pervaporation Dehydration of Acetic Acid (English)

WU Xiao-Wei, GUI Tian, YAN Zhi-Cheng, LI Yu-Qin, CHEN Xiang-Shu

DOI:10.11862/CJIC.2021.163
Chinese J. Inorg. Chem., **2021**,**37**(8):1482-1492

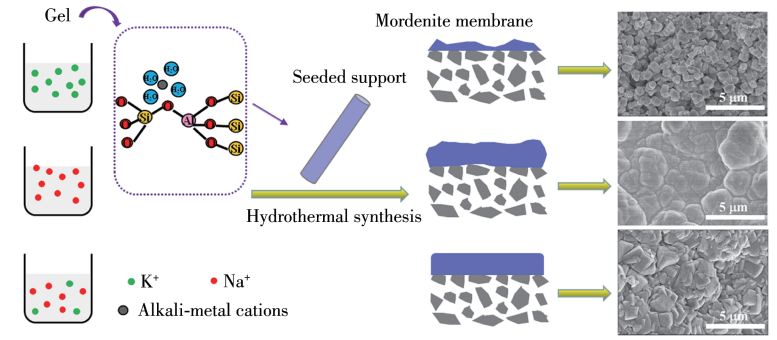

Na^+ had a significant acceleration effect on mordenite crystallization while Li^+, K^+ and Cs^+ showed a slower crystallization rate, and compact mordenite membranes prepared with the n_{Na^+}/n_{K^+}=2 in synthesis gel displayed good hydrophilicity.

Palladium-Based Coordination "Clips" with Carboxamide-Pyrazolate Ditopic Ligands: Self-Assembly and Catalytic Properties (English)

HU Xiao-Peng, WANG Zhi-Feng, YU Shu-Yan

DOI:10.11862/CJIC.2021.159
Chinese J. Inorg. Chem., **2021**,**37**(8):1493-1503

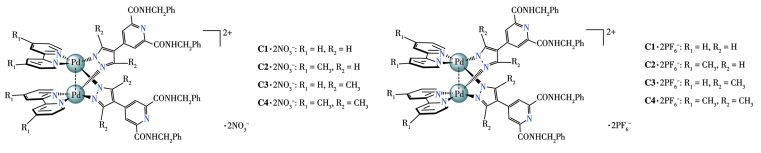

Two series of cationic dinuclear supramolecular **C1**·NO_3^-~**C4**·$2NO_3^-$ and **C1**·$2PF_6^-$~**C4**·$2PF_6^-$ were synthesized from two novel ditopic carboxamide-pyrazolate ligands via a directed self-assembly process in aqueous solution. All these clip-like dipalladium(Ⅱ) complexes exhibited highly catalytic activities towards Suzuki-coupling reaction under mild conditions.

Syntheses, Spectroscopic Properties and Terahertz Time Domain Spectroscopy of Two Copper(I) Complexes Based on Diphosphine Ligands and N-Donor Ligands (English)

LI Zi-Xi, HU Cong, SUN Zhen-Zhou, LI Xiao-Qi, HAN Hong-Liang, YANG Yu-Ping, XIN Xiu-Lan, JIN Qiong-Hua

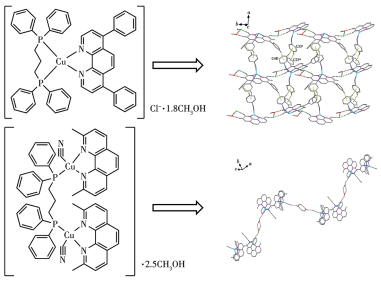

An asymmetric unit of complex **1** consists of one [Cu(dppp) (Bphen)]Cl·1.8CH_3OH and the asymmetric units form a 2D net structure through four hydrogen bonds, as well as three C—H $\cdots\pi$ molecular interactions. Complex **2** forms a 1D infinite chain through two hydrogen bonds. The fluorescence spectra and terahertz time-domain spectroscopy of both the complexes were studied.

DOI:10.11862/CJIC.2021.175
Chinese J. Inorg. Chem., **2021**,**37**(8):1504-1512

Two-Dimensional Luminescent Coordination Polymer Based on Dinuclear $\{Zn_2(COO)_4\}$ Second Buildings Units: Crystal Structure and Detection of Fe^{3+} (English)

HUANG Jia-Xiang, ZHAO He, LIU Shu-Qin, ZHANG Jian-Jun

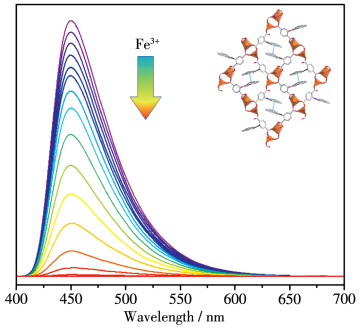

A coordination polymer with a (4,4) network topology exhibited good selective detection of Fe^{3+}.

DOI:10.11862/CJIC.2021.155
Chinese J. Inorg. Chem., **2021**,**37**(8):1513-1518

Improving Energy Barrier by Altering Coordination Environment in Two Dy(Ⅲ) Single-Ion Magnets (English)

ALI Basharat, LI Xiao-Lei, TANG Jin-Kui

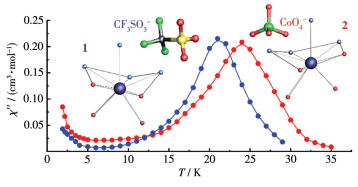

Alteration in the axial bond parameters through tuning the synthesis strategy results in distinct relaxation energy barriers of two analogous Dy-SIMs single-ion magnets.

DOI:10.11862/CJIC.2021.174
Chinese J. Inorg. Chem., **2021**,**37**(8):1519-1526

Errata

Correction to "Synthesis and Characterization of Metal-Organic Framework Based on 2,6-Bis(4-carboxybenzylidene) cyclohexanone"

PAN Wei, MA Chi-Xiao, ZHOU Chuan-Jiang, ZHANG Lu, ZHANG Jun-Yong, SHI Yan-Bo, XU Hao, ZHU Dun-Ru, XIE Jing-Li

DOI:10.11862/CJIC.2021.169
Chinese J. Inorg. Chem., **2021**,**37**(8):1527-1528